Biologics: Targets and Therapy

Dovepress
Taylor & Francis Group

Open Access Full Text Article

ORIGINAL RESEARCH

Therapeutic Potential of Compounds with High Affinity to BAG2 in Inhibiting Keloid Disease

Yinmin Wang*, Zhaoqi Yuan*, Renpeng Zhou*, Lin Lu, Xiuxia Wang, Jun Yang

Department of Plastic and Reconstructive Surgery, Shanghai Ninth People's Hospital, Shanghai Jiao Tong University, School of Medicine, Shanghai, People's Republic of China

*These authors contributed equally to this work

Correspondence: Xiuxia Wang; Jun Yang, Department of Plastic and Reconstructive Surgery, Shanghai Ninth People's Hospital, Shanghai Jiao Tong University, School of Medicine, 639 Zhi Zao Ju Road, Shanghai, People's Republic of China, 200011, Tel +8621-23271699-5118, Email wangxiuxia_hi@126.com; yj55569@hotmail.com

Purpose: Targeting the distinct genetic and protein expression profiles of keloids necessitates the identification of novel therapeutic targets. This study was aimed to elucidate the role of Bcl-2-associated athanogene 2 (BAG2) in keloid pathology and identify compounds with high-affinity to BAG2.

Patients and Methods: Cell migration, and cell proliferation assays, along with flow cytometry, were used to evaluate the effects of BAG2 on keloid fibroblasts (KFs) derived from tissue samples of patients with abdominal or chest keloids. Additionally, histological examinations and Western blotting were performed to investigate BAG2's role in keloids. Surface plasmon resonance (SPR) was employed to identify compounds with high-affinity to BAG2, and the effects of these compounds on keloids was assessed.

Results: Inhibition of BAG2 significantly decreased collagen deposition, cell proliferation and migration in keloid tissues. The modulatory effect of BAG2 on these processes appears to be mediated partly by the MEK signaling pathway. Among the tested compounds, Bazedoxifene acetate and Ponesimod showed high affinity for BAG2 and demonstrated a more pronounced inhibitory effect on collagen deposition of the keloid tissues than other candidates.

Conclusion: This study revealed the pathogenic role of BAG2 in keloid and identified compounds with high-affinity to BAG2, Bazedoxifene acetate and Ponesimod. The therapeutic capabilities of these compounds demonstrated their potential to improve therapeutic strategies for localized, targeted treatment to keloids.

Keywords: keloids, BAG2, targeting therapy, surface plasmon resonance, bazedoxifene acetate

Introduction

As a benign disease, keloids are featured by the overgrowth of dense fibrous tissue on the affected skin. Although benign, they often cause troublesome symptoms including itching, pain, and pruritus. Furthermore, their high recurrence rates make them particularly challenging in clinical practice.[1] Recommended treatments for keloids include compression therapy, intralesional injections, laser therapy, topical treatments, surgical excision, postoperative radiotherapy, and cryotherapy.[2] However, the nonspecific nature of these therapies increases the risk of damaging surrounding tissues. Intralesional corticosteroid injections, a standard first-line treatment, frequently result in side effects such as localized pain and changes in skin appearance.[3] The combination of corticosteroids and 5-Fluorouracil has demonstrated potential in improving treatment outcomes, yet persistent side effects remain a concern.[4] Furthermore, irregular post-operative radiotherapy, or intralesional injections, and high-risk sites have also been implicated in the recurrence of keloids.[5–7] Therefore, targeting the distinct genetic and protein expression profiles of keloids compared to normal skin necessitates the identification of novel therapeutic targets and corresponding ligands to advance keloid treatment.[8]

Previous studies on keloid therapy have primarily focused on the transforming growth factor-beta (TGF-β)/Smad signaling pathway,[9,10] which plays a crucial role in the prolonged stimulation of fibroblasts and myofibroblasts, leading to excessive collagen production in keloids.[9] However, considering the involvement of TGF-β in multiple biological processes, therapies

Received: 3 June 2025
Accepted: 9 August 2025
Published: 24 August 2025

targeting this signaling may cause systemic cytotoxic effects, limiting the advancement of TGF-β-based treatments for fibrotic diseases.[10] Therefore, further research is warranted to refine targeted therapies for keloids.

In our previous study, we identified several potential targets for keloid therapy through Mendelian randomization and single-cell sequencing analyses. However, these studies did not reveal any functional targets. Notably, proteins from the BAG family have attracted our interest due to their overexpression in both tumors and, to some extent, keloids, highlighting the tumor-like properties of these lesions.[11] Among them, BAG cochaperone 2 (BAG2) has emerged as a promising target for keloid therapy according to the single-cell sequencing analysis. Previous research has shown that the high BAG2 expression among tumor-associated fibroblasts correlated with the poor prognosis in breast cancer and its anti-apoptotic characteristics,[12,13] suggesting that BAG2 may play a similar role in keloid progression. Mechanistically, BAG2 negatively regulates the chaperone-associated ubiquitin ligase, C terminus of Hsc70-interacting protein (CHIP), which facilitates the ubiquitin-mediated degradation of misfolded proteins. This suggests that BAG2 may inhibit the degradation of specific proteins, including overexpressed collagen in keloids. Additionally, BAG2 interacts with the MAPK signaling pathway, influencing downstream cellular proliferation.[14,15] In keloids, BAG2 may inhibit collagen degradation and promote abnormal collagen accumulation, warranting further investigation.

This study aimed to validate the role of BAG2 in keloid progression and identify compounds targeting BAG2, employing high-throughput screening technology tailored for keloid patients. The experimental setup is illustrated in Figure S1. Additionally, we explored the intrinsic connection between BAG2 and the progression of keloids to provide insights for more precise keloid management.

Materials and Methods

Ethics Statement

Keloid biopsies (10 patients with 4 men and 6 women age ranging from 26 to 42 years old, with keloids from operative excision of previous abdominal incisionor chest incision, having the lesion of over one year without reduction, without previous surgical treatment or radiotherapy, diagnosed by 2 experienced clinical experts with lesions extending beyond the wound boundary into the normal skin and other clinical features) and normal skin samples (3 female patients, aged 38, 41 and 42, with skin excision from facial plastic surgery as brow lifting) were obtained from the Shanghai Jiao Tong University affiliated ninth people's hospital in accordance with the institutional review board (SH9H-2024-TK561). All patients provided formal, informed and written consent to supply a biopsy for this study. The study complied with the Declaration of Helsinki.

Keloid Fibroblasts (KFs) Isolation and Culture

Ten keloid samples from four men and six women were obtained after surgical excision. The sterile samples were rinsed in PBS, cut into pieces, and digested with 0.2% collagenase IV for 4 hours at 37 °C. After centrifugation, the sedimentary cells were resuspended in DMEM supplemented with 10% fetal bovine serum (FBS), 100 U/mL penicillin, and 100 μg/mL streptomycin, and incubated at 37°C in a 5% CO_2 incubator. The spindle keloid fibroblasts (KFs) from at least three patients at passages 2 to 3 were mixed for usage in further experiments.[16]

Single-Cell Data Analysis

To explore BAG2 gene expression in different cell groups, we downloaded the single-cell dataset GSE181297 of keloid patients from the Gene Expression Omnibus (GEO) database.[17] This dataset was generated via the Illumina NovaSeq 6000 platform for scRNA-seq including keloid and normal skin samples from human subjects. The data processing included normalizing, filtering low-quality cells, de-batching, selecting highly variable genes for dimensionality reduction, and analyzing BAG2 expression in different cell clusters.

Quantitative Real-Time Polymerase Chain Reaction (qRT-PCR)

qRT-PCR was performed as previously described.[18] Briefly, total RNA was extracted from cells after treatment using an RNA isolation kit (Takara Bio, Shiga, Japan). RNA purity was assessed by measuring the A260/A280 ratio, with acceptable values ranging from 1.8 to 2.0. The primers used for gene amplification are listed in Table 1. The results from three independent reactions were used to determine relative gene expression, normalized against β-actin expression.

Table 1 Primer Sequence

Primer Name	Sequence (5' - 3')	Target Gene
M0018f	5' AGG GCC AAG ACG AAG ACA TC 3'	Human *COL1A1*
M0018r	5' GTC GGT GGG TGA CTC TGA GC 3'	
M0005f	5' TAC TAC GCC AAG GAG GTC AC 3'	Human *TGFB1*
M0005r	5' GAG AGC AAC ACG GGT TCA G 3'	
M0323f	5' GAA GTC AAC CAG ACC ACC TTA T 3'	Human *TIMP1*
M0323r	5' GAA GTA TCC GCA GAC ACT CTC 3'	
M0009f	5' AAG GTG ACA GCA GTC GGT T 3'	Human *ACTB*
M0009r	5' TGT GTG GAC TTG GGA GAG G 3'	

Cell Transfection

Small interference RNA (si-RNA) targeting BAG2 for BAG2 knockdown and its negative control (si-NC) were synthesized by Sangon Biotech (Shanghai, China). The sequence of si-BAG2 was listed in Supplementary Table 1. The non-transfected KFs were set as controls. Cell transfection was conducted using RNATransMate transfection reagents (Sangon Biotech, Shanghai, China) according to the manufacturer's protocol.

Lentiviral Production and Infection

DNA oligonucleotides encoding primers for obtaining the target gene BAG2 (sequences: BAG2-1, 5'-AGGTCGACT CTAGAGGATCCCGCCACCATGGCTCAGGCGAAGATCAACGCTAAAG-3', BAG2-2, 5'-TCCTTGTAGTCCATGGA TCCATTGAATCTGCTTTCAGCATTTTG-3'), or a negative control were inserted into the lentiviral vector GV703 (Genechem, Shanghai, China). Human mRNA-BAG2 cDNA (synthesized by Genechem, Shanghai, China) was inserted into the BamHI/Age I sites of the lentiviral vector GV703. For lentiviral production, 293T cells were transfected with the lentiviral vector along with packaging plasmids using Lipofectamine 2000 (Life Science, USA) according to the manufacturer's instructions. At 48 h and 72 h after transfection, culture media was collected, pooled and filtered. Human Fibroblast cell line (HHF1) obtained from The Institute of Cell Biology, Chinese Academy of Sciences was infected with the indicated lentivirus, and BAG2 expression was determined by WB at 48 h after infection.

Ex-Vivo Explant Culture of Keloid Tissue

After harvesting aseptic keloid tissue, and removing epidermis, the remaining dermis of keloids was cut into about 3×2 × 2 mm pieces by a scalpel. The dermal fragments were divided into different groups, and cultured for 3 days in DMEM containing 10% FBS as previously described.[19] After tissue attachment, the medium was replaced for the control, siRNA-treated, and compounds-treated groups, which were then incubated for an additional five and seven days. The explants were collected after treatment.

Cell Proliferation Assay

The KFs transfected with si-BAG2 and si-NC (2×10^3 cells/well) were seeded into a 96-well plate. Following the manufacturer's protocol, 10 μL of CCK-8 reagent (Beyotime, Shanghai, China) was added to each well and incubated for 2 hours at 37°C. Subsequently, cell proliferation was assessed daily from day 1 to day 5. The number of cells was quantified by measuring absorbance at 450 nm using a microplate reader. Each treatment group was evaluated in triplicate to ensure reliable results.

Cell Cycle Analysis

KFs were treated with si-BAG2, C16-PAF (Targetmol, #T21547, 10 nM), or si-BAG2 alone for 24 and 48 hours, along with the si-NC control. After treatment, the cells were rinsed once with PBS, and fixed with 70% ethanol overnight. The cell cycle analyses were performed according to the instructions of the Cell Cycle Kit (Qihai Biotechnology, Shanghai,

China), and flow cytometric analyses were performed by a flow cytometer (Beckman Coulter) equipped with ModiFit LT v2.0 software.

Cell Migration Assay

To evaluate the effect of BAG2 knockdown on the KFs migration, a scratch assay was performed. KFs were seeded in multi-well plates and cultured to confluence. The culture medium was then removed, and the cell monolayers were scratched using a 200 μL pipette tip. The cells were rinsed with PBS and subsequently treated with either si-BAG2, si-NC, or control. Images of cell migration were captured at 0 and 24 hours using an inverted light microscope (TE2000 Nikon, Japan) at 40×magnification at 0 and 24 hours. These experiments were performed in triplicate, and migration areas were quantified using ImageJ analysis software (National Institutes of Health, Bethesda, MD).

Histological, Immunohistochemical and Immunofluorescence Analyses

Keloid tissue and explant samples were fixed overnight in 4% paraformaldehyde at 4°C, embedded in paraffin, and sectioned to 5 μm thickness. The sections were subsequently stained with hematoxylin and eosin (H&E) and Masson's trichrome for histological examination. Furthermore, keloid tissue sections were also treated with antibodies specific to BAG2 and α-SMA at dilutions from 1:2000 to 1:100. Antibody binding was visualized using 3,3'-diaminobenzidine (DAB) chromogen (Dako, Glostrup, Denmark) and counterstained with hematoxylin for immunohistochemical analyses. For immunofluorescence staining, after overnight incubation with primary antibodies, specimens were incubated with secondary antibodies for 1 hour. Cell nuclei were stained with 4,6-diamidino-2-phenylindole (DAPI). Finally, digital images were obtained using a V10-ASW 4.2 computerized image analysis system (Olympus, Tokyo, Japan). The antibodies used were: BAG2 antibody (Affinity, #DF2650, 1:100), Goat Anti-Rabbit IgG (H+L) HRP (Jackson, #111-035-045, 1:200), α-SMA antibody (Proteintech, #67735-1-Ig, 1:100), Goat Anti-Mouse IgG (H+L) Red (Jackson, #115-295-003, 1:200), and Goat Anti-Rabbit IgG (H+L) FITC (Jackson, #111-095-003, 1:200). The positive rate of BAG2 was defined as the proportion of BAG2-positive cells among all the cells in the field.

Western Blot

Western blot was performed on tissue samples or cultured cells as indicated. Total protein was extracted using RIPA lysis buffer, as previously described.[18] The protein concentration of each lysate was determined using a BCA protein assay kit. Protein samples were separated by SDS-PAGE electrophoresis and transferred onto polyvinylidene fluoride (PVDF) membranes. The membranes were then blocked with 5% skimmed milk and immunoblotted with specific primary antibodies, including COL1, COL3, α-SMA, MEK, p-MEK and β-actin, diluted between 1:2000 and 1:1000 in TBST. After overnight incubation with the primary antibodies and three subsequent TBST washes, the membranes were incubated with the appropriate secondary antibodies for 1 hour at room temperature. Protein bands were detected using an enhanced chemiluminescence (ECL) kit (Amersham Biosciences, Chalfont St. Giles, UK). The intensity of each protein band was normalized against the β-actin band for comparison. The primary antibodies used in this study were: COL3 (Abcam, #Ab184993, 1:1000), COL1 (Huabio, #HA722517, 1:1000), α-SMA (Affinity, #AF1032, 1:1000), BAG2 (Affinity, #DF2650, 1:1000), MEK (Affinity, #AF3385, 1:1000), p-MEK (Affinity, #AF6385, 1:1000), and β-actin (Affinity, #AF7018, 1:2000).

Surface Plasmon Resonance (SPR) for Affinity Screening and Affinity Determination

SPR experiments were performed in at 25 °C on a BIAcore T200 with CM5 sensor chips, and data were analyzed with BIAcore T200 Evaluation software (GE Healthcare), following the manufacturer's instruction. BIAcore T200 optical biosensor was used to screen for BAG2 affinity and to measure equilibrium dissociation constant (K_D) values for protein–ligand interactions. A cell on the CM5 sensor chip was activated using a mixture of 200 μM 1-ethyl-3-(3-dimethylaminopropyl) carbodiimide and 50 μM N-hydroxysuccinimide at a flow rate of 10 μL/min for 420 seconds. Subsequently, BAG2 protein (50 μL) was mixed with 180 μL of 10 mM sodium acetate solution at pH 5.0 and immobilized on the cell surface at the same flow rate and duration for two cycles as previously described.[20] The cell was then blocked using 1 M ethanolamine. A neighboring channel, used as a reference, underwent the same activation and blocking steps, except immobilization was carried out with PBS adjusted to pH 5.0. Both channels were equilibrated

with PBS afterward. Grouped SPR single concentration screening: Fifty compounds were grouped, with each compound contributing 1 μL, combined in an EP tube to total 50 μL. EP tubes were labeled from 1 to 54, and 950 μL of PBS was added to achieve a screening concentration of 10 μM for each compound. The DMSO content was maintained at 5% within the correction range. Each run flowed at 10 μL/min for 150 seconds. After each run, the chip was regenerated for 5 minutes with 10 mM glycine-HCl (pH 2.0), repeating until all groups (54 in total) were tested. Sequential SPR single concentration screening: The two groups with the highest RU values from the first screening round (100 compounds total) were selected. Each compound was taken as 2 μL from the plate and mixed with 198 μL of PBS to achieve a screening concentration of 100 μM. Each run flowed at 10 μL/min for 150 seconds. At the end of each run, the chip was regenerated for 5 minutes with 10 mM glycine-HCl (pH 2.0) solution, repeating this process until all compounds (100 in total) were completed. Data were collected from the sample cell using BIAcore T200 Control software (v. 2.0, GE Healthcare) and normalized against the reference cell. Association and dissociation constants were calculated using global fitting to a 1:1 Langmuir binding model with BIAcore T200 Evaluation software (v. 2.0, GE Healthcare). Final figures were generated using Origin 7 software (v. 7.0552, OriginLab).

To determine the K_D value for protein-ligand interactions, each compound was diluted 6 times from 12 μM to 15.625 nM. The compounds were flowed over a chip with immobilized BAG2 protein from lowest to highest concentration at 10 μL/min for 150 seconds. After each concentration, the chip was regenerated with 10 mM glycine-HCl (pH 2.0) for 5 minutes at the same flow rate. Data were recorded in real time, with molecular weight adjustment and solvent correction applied to address non-specific binding and signal drift molecular effects. Data analysis was conducted using BIAcore T200 software (GE Healthcare) following the manufacturer's guidelines.

Statistical Analysis

All data are presented as means ± SD and analyzed using GraphPad Prism version 8 software (GraphPad Software Incorporation, La Jolla, California, United States). The cell migration area data were analyzed using Image J software. Sample sizes were determined based on practical and experimental considerations, without predetermined statistical methods. Differences among multiple groups were analyzed using analysis of variance (ANOVA), followed by Tukey's post hoc test for comparisons between groups ($\alpha = 0.05$). Differences among two groups were analyzed using *t*-test. Statistically significant differences were indicated by asterisks, with a two-tailed p-value of less than 0.05 considered significant.

Results

Higher BAG2 Expression in KF Clusters Compared to Normal Skin and Higher BAG2 Protein Expression in Keloid Tissue

After quality control of the GSE181297 dataset, we conducted dimensionality reduction and clustering analysis. Unique molecular identifiers between 200 and 6000 were selected. Cell clusters were categorized based on original molecular markers. These clusters included endothelial cell (EC), fibroblast (FB), proliferating myofibroblast (MFB), keratinocyte (KC), immune cells (lymphocytes, macrophages, and mast cells), lymphatic endothelial cell (LEC), and neural cell (Figure S2A and B). Besides, elevated BAG2 gene expression in KFs was observed in differential expression analysis (Figure S2C), with no significant difference in BAG2 expression between ECs and LECs in keloid and normal skin samples. Immunohistochemical staining confirmed BAG2 expression around fibrous nodules (Figure 1A). Additionally, immunofluorescent staining showed colocalization of BAG2 with α-SMA-positive cells, while BAG2 expression was also observed in α-SMA-negative cells, consistent with single-cell sequencing results (Figure 1B). Western blot analysis further demonstrated that BAG2 protein levels were significantly higher in keloid tissue than in normal skin samples (Figure 1C). The images of individual channel of immunofluorescence staining of keloid samples were showed in Figure S3A. The negative controls of immunohistochemical staining for keloid and normal skin, and the Hematoxylin and Eosin Staining of the keloid tissue was showed in Figure S3B and Figure S4.

 https://doi.org/10.2147/BTT.S533286

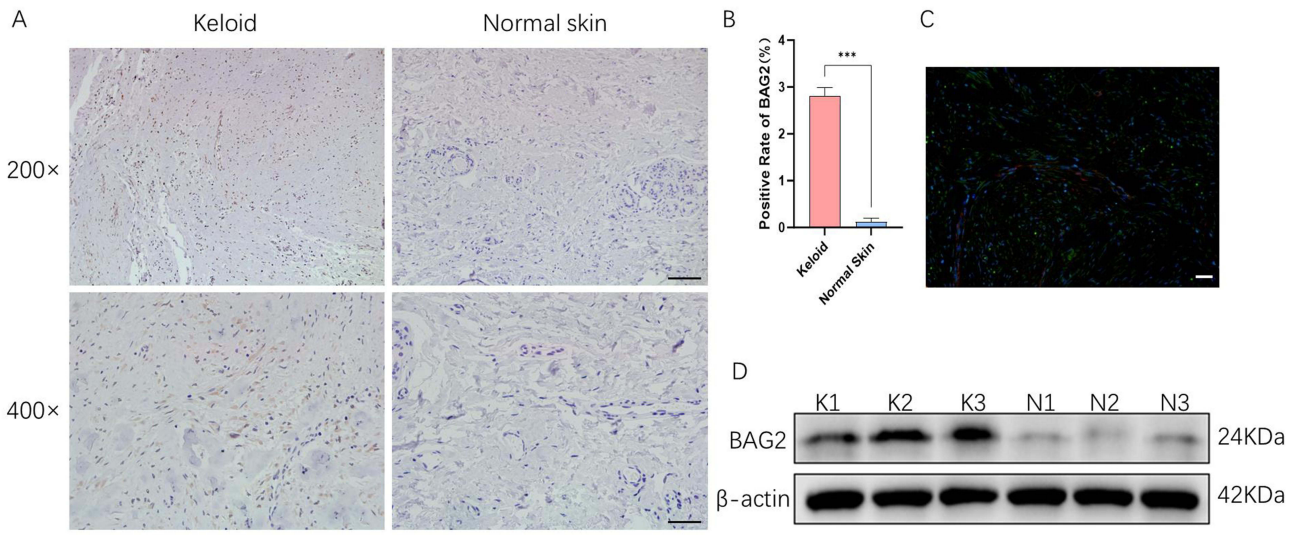

Figure 1 The expression of BAG2 in keloid and normal skin samples. (**A**) Immunohistochemical analysis reveals enhanced positive staining for BAG2 in and around the fibrous nodules of keloid tissues compared to normal skin samples. (Scale bar = 100 μm at 200× magnification; Scale bar = 50 μm at 400× magnification); (**B**) The statistical analysis of BAG2 protein expression in keloid tissues and normal skin samples, as detected by immunohistochemical staining; (**C**) Immunofluorescence staining of a keloid sample slide shows nuclear staining with DAPI (blue) and colocalization of BAG2 (green) with α-SMA (red) positive cells; BAG2 expression is also visible in α-SMA negative cells. (Scale bar = 100 μm); (**D**) BAG2 protein levels in keloid tissue were significantly elevated compared to normal skin samples. (K: Keloid; (N) Normal Skin). ****P<0.001*.

Inhibition of BAG2 Reduced Collagen Synthesis and Deposition of KFs, and in an Ex-Vivo Model

The relative gene expression of collagen type I (COL1), which is associated with collagen synthesis and excessive deposition in keloids,[21] and Tissue inhibitor of metalloproteinase 1 (TIMP1), which inhibits matrix metalloproteinases and subsequently promotes COL1 deposition in keloids,[19] was significantly decreased following BAG2 inhibition (Figure 2A). Additionally, Western Blot analysis showed reduced protein expression of BAG2, COL1, collagen type III (COL3), and α-SMA in si-BAG2-treated KFs, highlighting the role of BAG2 in abnormal collagen deposition (Figure 2B). Consistent with these findings, collagen structures in si-BAG2-treated ex-vivo keloid explants appeared thinner and more degraded compared to the control group (Figure 2C). Furthermore, COL1 and COL3 protein levels were significantly reduced in ex-vivo explants treated with si-BAG2 (Figure 2D).

Inhibition of BAG2 Reduced Migration and Proliferation of KFs, Correlating with the MEK Pathway

BAG2 inhibition significantly reduced the migration and proliferation of KFs (Figure 3A and B). Additionally, the relative gene expression of TGF-β, an indicator of the proliferation and migration of KFs, was significantly decreased in si-BAG2-treated KFs (Figure 3C).[22] In addition, Western Blot further demonstrated decreased levels of phosphorylated MEK (p-MEK) following si-BAG2 treatment (Figure 3D). Furthermore, si-BAG2 treatment significantly increased KFs' percentage within the G0/G1 phase, suggesting cell cycle arrest. This effect was reversed by C16-PAF, an MEK activator, which restored G0/G1 phase percentages in si-BAG2-treated KFs (Figure 3E).

Screening of Compounds with High-affinity to BAG2 via Surface Plasmon Resonance (SPR) and Their Cell Inhibition Rates

BAG2 protein was found to play a significant role in collagen deposition in keloid tissues and the proliferation of KFs, making it a potential target for keloid treatment. To explore compounds with high-affinity to BAG2, the structure of BAG2 predicted by AlphaFold3 is shown in Figure S5. SPR was employed as an affinity screening technology to identify potential high-affinity compounds for BAG2.

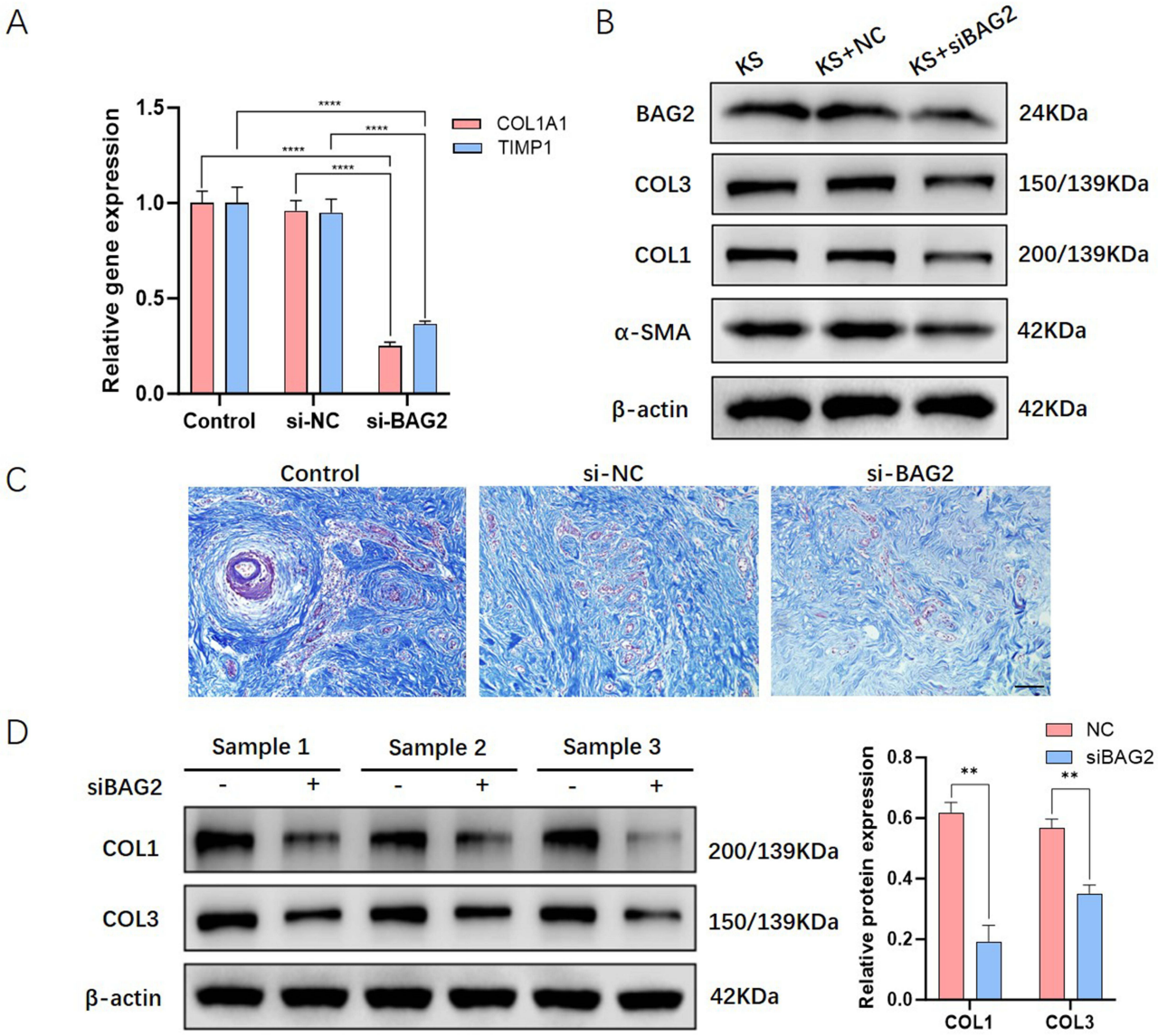

Figure 2 Inhibition of BAG2 reduced keloid collagen synthesis and deposition. (**A**) The relative gene expression of *COL1A1* and *TIMP1* in si-BAG2-treated keloid fibroblasts compared to control groups. Gene expression related to collagen synthesis and the inhibition of collagen degradation was significantly reduced following BAG2 inhibition; (**B**) Western blot analysis showing reduced protein expression of BAG2, COL1, COL3, and α-SMA in si-BAG2-treated keloid fibroblasts; (**C**) Masson's trichrome staining of keloid explants from different groups. Collagen structures in the si-BAG2-treated groups appeared thinner compared to control groups; (**D**) Western blot analysis demonstrates decreasing protein expression of COL1 and COL3 in si-BAG2-treated ex-vivo keloid explants. The reduction in COL1 and COL3 protein expression was statistically significant. Statistical analysis of relative protein expression is provided (n=3). ***P<0.01,* ***** *P<0.0001*.

A total of 2,732 compounds from the FDA and anti-fibrosis libraries were screened (Supplementary Table 2). In the first round, 2 groups of compounds were identified, and 6 compounds were identified as putative BAG2 ligands in the second round (Figure 4A and B). The primary cell inhibition rates of these 6 compounds on KFs were determined via CCK8 assays on Day 3 (Supplementary Table 3). Three compounds (Saikosaponin B1, Bazedoxifene acetate, and Ponesimod) showed significant inhibition of KFs and were selected for further investigation. Subsequently, the affinity index (K_D values) of these compounds with BAG2 was determined using SPR, and their inhibitory effects on KFs were evaluated at varying concentrations. The results indicated that Saikosaponin B1, Bazedoxifene acetate, and Ponesimod had K_D values of 6.35E−7 M, 2.84E−6 M, and 5.87E−6 M, respectively. Additionally, the fitted curves demonstrating the effects of different compound concentrations on the relative cell viability of KFs revealed IC50 values of 9.32 μM for Bazedoxifene acetate and 24.96 μM for Ponesimod, indicating that both drugs exhibit strong binding affinity and inhibitory effects (Figure 4C and D). Although Saikosaponin B1 exhibited relatively high binding affinity to BAG2, its inhibitory effect on KFs was below 40% at

https://doi.org/10.2147/BTT.S533286

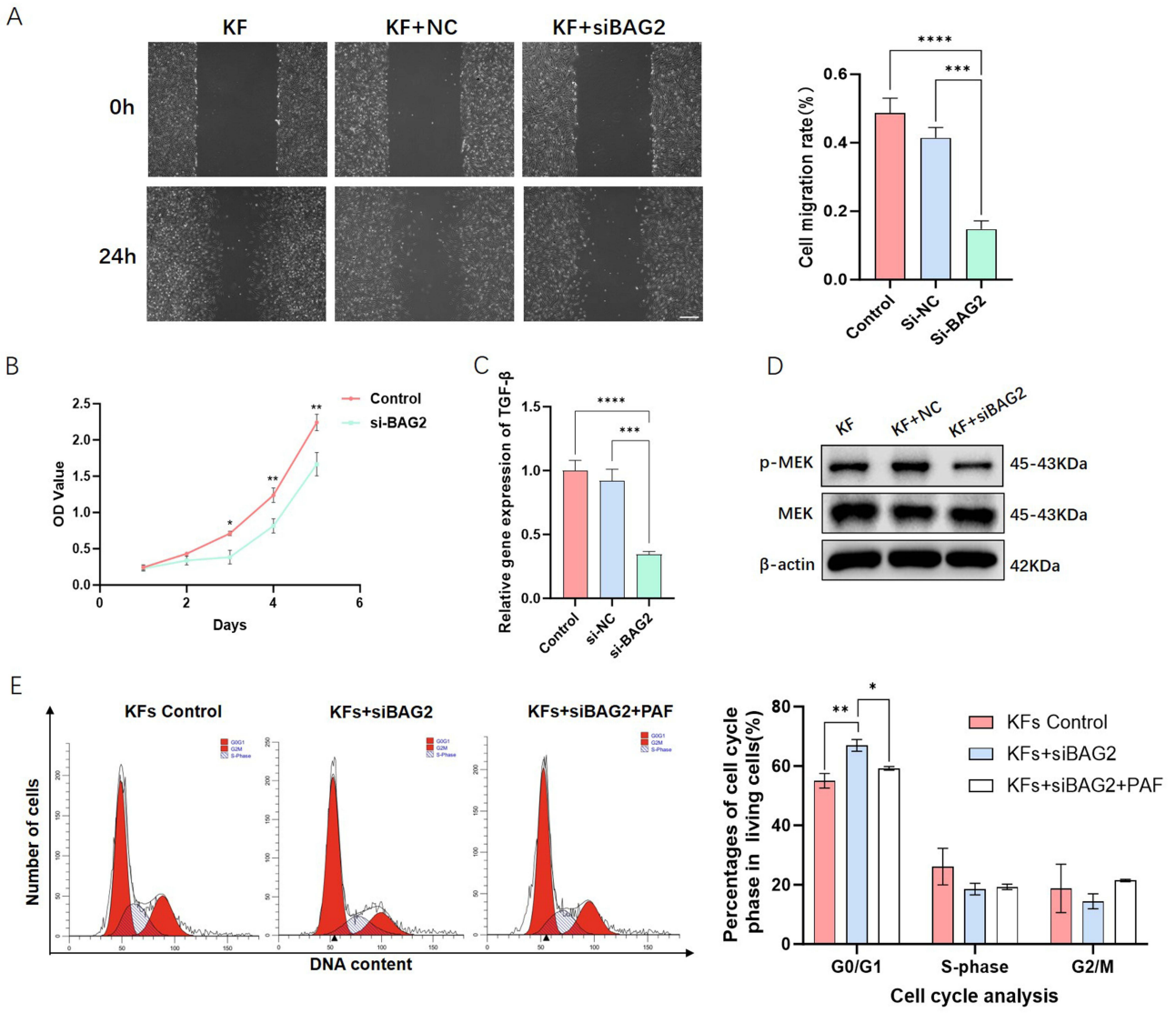

Figure 3 Inhibition of BAG2 reduced KF migration and proliferation via the MEK signaling pathway. (**A**) Representative images and bar graph depict the migration of KFs treated with or without si-BAG2 at 0 and 24 hours after scratching (n=3). Scale bar = 500 μm; (**B**) CCK-8 assays were performed on control and si-BAG2-treated KFs, showing a significant reduction in the proliferation of si-BAG2-treated cells (n=3); (**C**) Relative gene expression of TGF-β in si-BAG2-treated and control KFs, with significantly decreased TGF-β expression observed following si-BAG2 treatment (n=3); (**D**) Western blot analysis revealing decreased p-MEK in si-BAG2-treated cells; (**E**) Representative cell cycle profiles of KFs from various groups, assessed by flow cytometry, accompanied by statistical analysis (n=3). **P<0.05, ** P<0.01, ***P<0.001, **** P<0.0001*. KF, keloid fibroblast.

a concentration of 50 μM (Figure S6), suggesting it is not an optimal candidate for BAG2 targeting. The association rate constants (Ka) and dissociation rate constants (Kd) of these compounds are listed in Supplementary Table 4. Overexpressing BAG2 in human fibroblasts, and adding Bazedoxifene (10μM) acetate or Ponesimod (25μM) for 48h, it was found that these two compounds could inhibit BAG2-mediated cell cycle transition and cell proliferation (Figure 4E). The overexpression of BAG2 was validated by Western blot (Figure S7).

Compounds with High-Affinity to BAG2 Exhibited Inhibition of Collagen Deposition in Keloid Tissue

To further evaluate the therapeutic effects of the identified compounds on keloids, the effects of Bazedoxifene acetate and Ponesimod were assessed through protein expression analysis of COL1 and COL3, as well as histological evaluation of ex-vivo keloid explants. The experiments revealed that treatment with Bazedoxifene acetate and Ponesimod for five days

 https://doi.org/10.2147/BTT.S533286

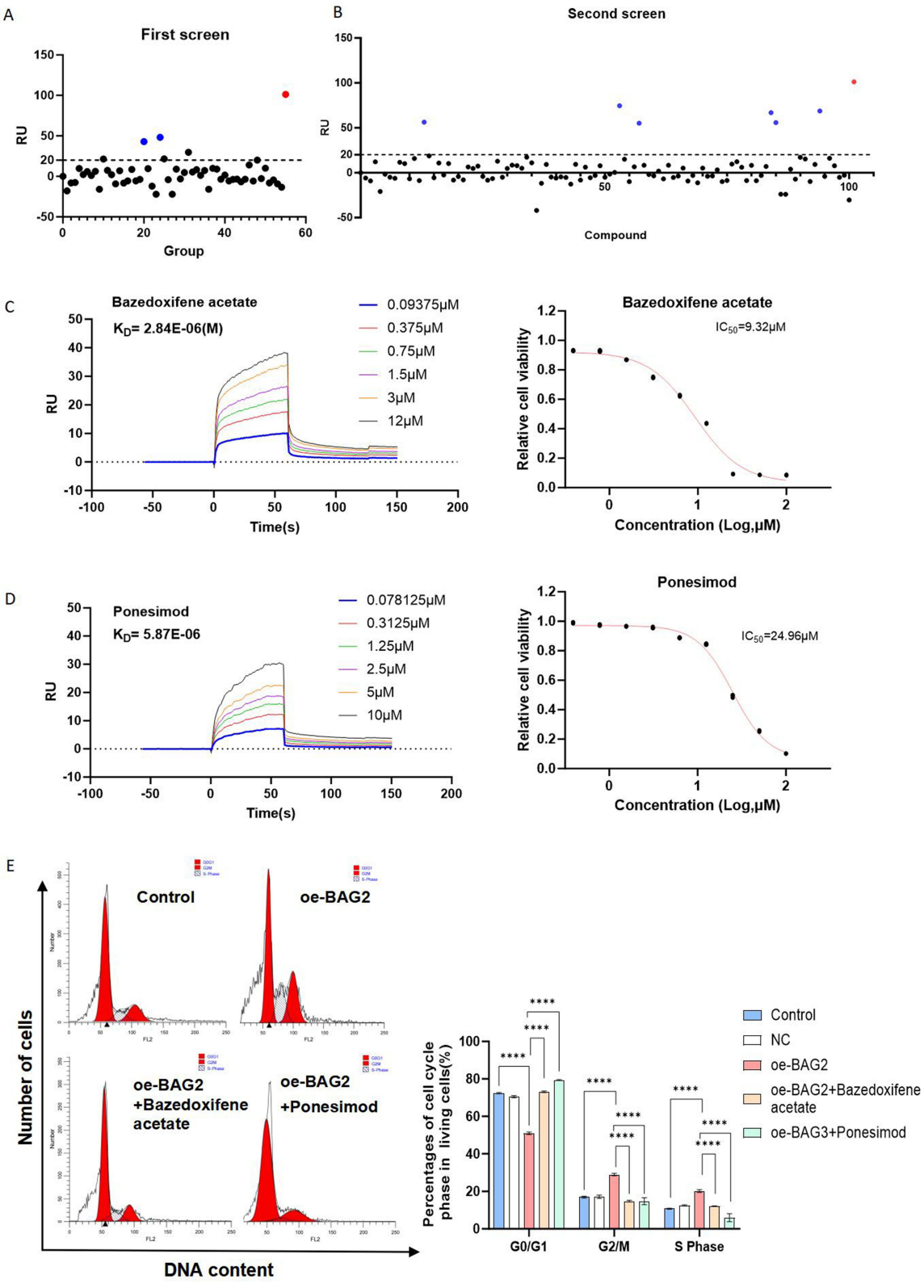

Figure 4 SPR screening of high-affinity compounds with BAG2 and validation in vitro. (**A**) Initial screening of 54 compound groups via SPR identified two groups demonstrating high affinity for BAG2 (shown in blue), compared to the positive control, BAG2 rabbit monoclonal antibody (mAb) from ABclonal Technology (A8775) (shown in red); (**B**) A second screening via SPR of two groups comprising 100 compounds revealed six compounds with high affinity for BAG2 (shown in blue), using the same BAG2 rabbit mAb as a positive control (shown in red); (**C-D**) SPR assays were used to analyze the binding affinities of Bazedoxifene acetate and Ponesimod to human BAG2 protein. Additionally, dose-response curves displaying the response of KFs to Bazedoxifene acetate and Ponesimod treatment over 72 hours are presented (n=6); (**E**) Representative cell cycle profiles of human fibroblasts from control, BAG2 overexpressed (oe-BAG2), oe-BAG2 treated with Bazedoxifene acetate or Ponesimod groups, assessed by flow cytometry, accompanied by statistical analysis (n=3). **** *P<0.0001*. KF, keloid fibroblast.

https://doi.org/10.2147/BTT.S533286

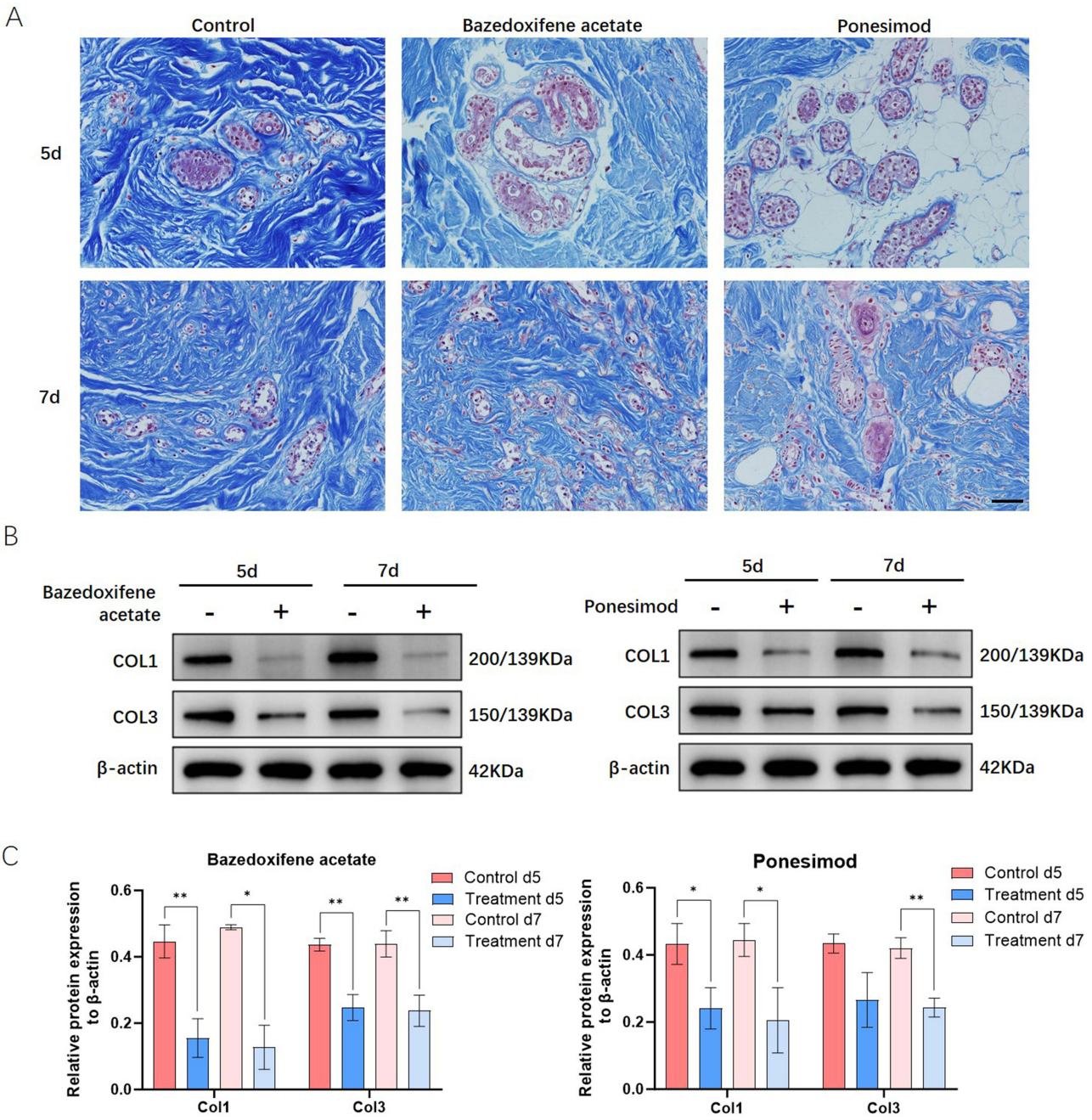

Figure 5 Masson's trichrome of keloid explants in different groups. (**A**) In ex-vivo keloid explants treated with Bazedoxifene acetate and Ponesimod, the collagen structures appeared thinner compared to control groups; (**B**) Western blot analysis showed reduced protein expression of COL1 and COL3 in ex-vivo keloid explants treated with Bazedoxifene acetate and Ponesimod. Notably, Bazedoxifene acetate demonstrated a superior inhibitory effect on collagen deposition; (**C**) Statistical analysis of the relative protein expression is included (n=3). **P<0.05, **P<0.01*.

or longer significantly reduced both the protein expression of collagen and the histological deposition of collagen in the ex-vivo explants (Figure 5). Additionally, Bazedoxifene acetate showed a superior inhibitory capacity for the expression of COL1 and COL3. These findings confirmed that compounds with high-affinity to BAG2 could markedly inhibit collagen deposition in ex-vivo keloid explants, indicating their clinical potential as therapeutic agents for keloids.

Discussion

Keloids, a benign fibrogenic skin disease, share numerous characteristics with tumors, including the absence of spontaneous regression, excessive proliferation, and high recurrence rates.[23] Consequently, it is critical to explore therapeutic agents that target specific mechanisms involved in keloid formation. In this study, we identified BAG2 as a novel therapeutic target and screened thousands of compounds to find high-affinity BAG2 ligands. Our findings include the identification of Ponesimod and Bazedoxifene acetate as high-affinity ligands to BAG2, whose inhibitory effects were evaluated on keloid explants.

The present study observed an upregulation of BAG2 in keloid tissues, meanwhile, decreasing BAG2 with siBAG2 inhibited the proliferation of KFs, which correlated with MEK signaling. Consistent with the alterations of TGF-β following BAG2 inhibition, TGF-β modulates cell proliferation through the MEK pathway via a Smad-independent signaling mechanism (Derynck et al, 2003). This is consistent with prior findings linking MEK pathway activation to the proliferation of KFs,[24] and to the proliferative and migratory behaviors of cancer cells.[25,26] As evidenced by our findings, si-BAG2 suppressed KFs' progression at the G0/G1 phase, a process that could be reversed by MEK activation. This indicates that BAG2 facilitates KF proliferation, which is correlated with the MEK signaling pathway, as an early indicator of a long-term process involving ECM remodeling. In accordance with previous studies, inhibiting the MEK pathway could induce G0/G1 phase arrest.[27,28] Additionally, the initial phosphorylation site Ser20, located within the curled helical domain near the amino terminus of BAG2, is phosphorylated by MAPKAPK-2. The p38 MAPK-MAPKAPK-2-BAG2 phosphorylation cascade, activated in response to extracellular stress, influences cell proliferation activities,[29] and may explain BAG2's role in activating the MEK pathway. The BAG2-Heat shock protein (HSP) complex maintains basement membrane integrity and regulates ECM and cell junctions in glial cells, suggesting a similar role in keloids.[30] BAG2 also has anti-apoptotic effects that promote cell survival and, in some cases, enhances TIMP synthesis and activity by boosting intracellular anti-apoptotic factors. Since TIMPs inhibit MMP activity to control ECM degradation, BAG2-mediated upregulation of TIMPs may reduce MMP-driven ECM breakdown, preventing excessive degradation.[13]

While the proliferation and migration of KFs are well-documented, accelerated collagen accumulation also plays a significant role in keloid pathology.[19] Additionally, mechanical stress at keloid sites has been recognized as a risk factor for the initiation and progression of this condition.[31] The stiffness of the extracellular matrix (ECM) in keloids, largely due to collagen accumulation, augments the effects of mechanical stress, which, in turn increases the production of ECM by KFs.[32] Therefore, halting the collagen deposition cycle is vital for effective keloid therapy.[33] Traditional therapies for keloids fail to adequately target the essential pathological processes of collagen synthesis and degradation.[34] In this study, altering BAG2 activity reduced both collagen synthesis and deposition in vitro and ex vivo. Additionally, our findings demonstrate that drugs with high-affinity to BAG2 can significantly reduce collagen accumulation, highlighting their potential as novel targeted therapies for keloids that inhibit collagen deposition and reduce the viability of KFs. In pulmonary fibrosis, TGF-β treatment promotes α-SMA expression through acetylated CCAAT/enhancer binding protein β (C/EBP-β), and a similar mechanism may exist in keloids, which warrants further investigations.[35]

Several skin diseases, including psoriasis, vitiligo, dermatitis, and skin cancers, have been successfully treated with targeted therapies.[36–39] Drugs such as vemurafenib and trametinib, which target the BRAF mutation and MEK respectively, have significantly advanced the field of targeted therapy, although many such drugs are still in the preclinical research stage. Specifically, drugs targeting keloids, due to their localized presence on the body surface, could offer more precise treatment options. Nevertheless, there are currently no specific inhibitors targeting BAG2, a keloid-associated marker identified through this study. In this study, several high-affinity BAG2 ligands with were identified, including Saikosaponin B1, Ponesimod, and Bazedoxifene acetate, and verified their capability to inhibit collagen expression and deposition in ex-vivo keloid tissue. Saikosaponin B1, a bioactive molecule found in Radix Bupleuri, has been shown to exhibit anticancer properties[40] and antifibrotic activity in liver fibrosis.[41] Ponesimod, a Sphingosine 1-phosphate (S1P) modulator, has been investigated as a treatment for Multiple Sclerosis, focusing on its ability to regulate S1P activity in lymphocytes.[42] Bazedoxifene acetate, a selective Estrogen Receptor modulator, was examined for its role as a BAG2 ligand and its capacity to inhibit the viability of KFs in this study.[43] Interestingly, tamoxifen, another Estrogen Receptor modulator, has also been shown to reduce keloid collagen fibers.[44] Like bazedoxifene acetate, tamoxifen's impact on keloids appears to extend beyond simple Estrogen Receptor

modulation. Bazedoxifene acetate appears to influence keloid pathology by correlating with the inhibition of BAG2. The mechanisms through which bazedoxifene acetate and ponesimod act on keloids necessitate further detailed exploration.

Despite the lack of prior reports on these drugs as keloid inhibitors, their strong affinity for BAG2 and effectiveness in inhibiting KFs suggest their potential as promising candidates for targeted keloid therapy. Bazedoxifene acetate, in particular, stands out for its lower K_D, lower IC_{50}, and higher binding affinity. As an FDA-approved medication, bazedoxifene acetate may manage antifibrotic activity by affecting both collagen deposition and the viability of KFs. Moreover, due to their relatively high SLogP values, as detailed in Supplementary Table 5, bazedoxifene acetate and ponesimod were more likely to facilitate transdermal absorption, potentially reducing side effects associated with systemic administration. Topical application of these compounds may provide a viable therapeutic option for keloid treatment.

Despite the promising potential of drugs targeting BAG2 in keloid therapy, treatment with these agents may induce unintended off-target effects on other proteins. Therefore, further functional analyses and the development of systems to predict potential side effects are warranted. In this study, we found that inhibiting BAG2 could reduce collagen deposition. Additionally, the system of MMPs and TIMPs was also affected, warranting further investigation. Furthermore, the direct interaction between BAG2 and MEK signaling requires further investigation to elucidate the role of BAG2 in keloid formation. In addition, proliferation is a confounding factor for the scratch assay, the effect of BAG2 in the migration of KFs should be further investigated. Further, in vivo models are warrant for validation of the role of BAG2 in keloids. Compared to the ex-vivo model, the *in-vivo* model provides more comprehensive information on physiological responses and systemic pathological changes. In addition, as indicated by SPR, the binding affinity of Bazedoxifene acetate and Ponesimod to BAG2 is relatively higher than that of the other tested drugs. To further validate the effect of Bazedoxifene acetate and Ponesimod on keloids via BAG2, silencing experiments should be conducted in future studies. In summary, this study highlighted BAG2's impact on collagen deposition and the proliferation of KFs, which are critical to the pathogenesis of keloids, benign skin tumors with high recurrence rates. Additionally, we identified compounds with high-affinity ligands to BAG2 that could serve as potential therapeutic targets. Among the compounds tested, Bazedoxifene acetate demonstrated superior affinity for BAG2 and more effective inhibition of keloid fibroblasts and keloid tissue compared to other ligands, suggesting novel approaches for the precise management of keloid disease.

Conclusion

This study revealed the pathogenic role of BAG2 in keloid and identified its high-affinity ligands, Bazedoxifene acetate and Ponesimod. The therapeutic capabilities of these compounds demonstrated their potential to improve targeting therapy for keloids.

Resource Availability

The data underlying this article are available in the article and in its online supplementary material. Single cell sequencing data is available in [GEO database] at [https://www.ncbi.nlm.nih.gov/geo/query/acc.cgi?acc=GSE181297]. Further data underlying this article will be shared on reasonable request to the corresponding author.

Acknowledgments

We thank all the patients who provided samples for the experiment for their support. This work was supported by National Nature Youth Foundation of China (Grant No. 82402938 & 82102319) Science and Technology Commission of Shanghai Municipality (Grant No. 22MC1940300) and Wuxi Taihu Lake Talent Plan, Supports for Leading Talents in Medical and Health Profession. The funding body did not play a role in the study design, data collection, analyses, interpretation, manuscript preparation, and in the decision to submit the manuscript.

Author Contributions

All authors made a significant contribution to the work reported, whether that is in the conception, study design, execution, acquisition of data, analysis and interpretation, or in all these areas; took part in drafting, revising or critically reviewing the article; gave final approval of the version to be published; have agreed on the journal to which the article has been submitted; and agree to be accountable for all aspects of the work.

Disclosure

The authors have declared that no conflict of interest exists. The patents associated with this article include patent application number 202411342096.X, credited to Yinmin Wang, Lin Lu, and Jun Yang.

References

1. Naik PP. Novel targets and therapies for keloid. *Clin Exp Dermatol*. 2022;47(3):507–515. doi:10.1111/ced.14920
2. Walsh LA, Wu E, Pontes D, et al. Keloid treatments: an evidence-based systematic review of recent advances. *Syst Rev*. 2023;12(1):42. doi:10.1186/s13643-023-02192-7
3. Kim SW. Management of keloid scars: noninvasive and invasive treatments. *Arch Plast Surg*. 2021;48(2):149–157. doi:10.5999/aps.2020.01914
4. Jiang ZY, Liao X-C, Liu M-Z, et al. Efficacy and safety of intralesional triamcinolone versus combination of triamcinolone with 5-fluorouracil in the treatment of keloids and hypertrophic scars: a systematic review and meta-analysis. *Aesthetic Plast Surg*. 2020;44(5):1859–1868. doi:10.1007/s00266-020-01721-2
5. Ekstein SF, Wyles SP, Moran SL, et al. Keloids: a review of therapeutic management. *Int J Dermatol*. 2021;60(6):661–671. doi:10.1111/ijd.15159
6. Deng K, Xiao H, Liu X, et al. Strontium-90 brachytherapy following intralesional triamcinolone and 5-fluorouracil injections for keloid treatment: a randomized controlled trial. *PLoS One*. 2021;16(3):e0248799. doi:10.1371/journal.pone.0248799
7. Katano A, Minamitani M, Yamashita H. Risk factors for local recurrence of keloids and hypertrophic scars after postoperative electron beam radiotherapy. *J Cancer Res Ther*. 2024;20(1):163–166. doi:10.4103/jcrt.jcrt_1861_22
8. Deng CC, Hu Y-F, Zhu D-H, et al. Single-cell RNA-seq reveals fibroblast heterogeneity and increased mesenchymal fibroblasts in human fibrotic skin diseases. *Nat Commun*. 2021;12(1):3709. doi:10.1038/s41467-021-24110-y
9. Zhang T, Wang X-F, Wang Z-C, et al. Current potential therapeutic strategies targeting the TGF-β/Smad signaling pathway to attenuate keloid and hypertrophic scar formation. *Biomed Pharmacother*. 2020;129:110287. doi:10.1016/j.biopha.2020.110287
10. Peng D, Fu M, Wang M, et al. Targeting TGF-β signal transduction for fibrosis and cancer therapy. *Mol Cancer*. 2022;21(1):104. doi:10.1186/s12943-022-01569-x
11. Mariotto E, Viola G, Zanon C, et al. A BAG's life: every connection matters in cancer. *Pharmacol Ther*. 2020;209:107498. doi:10.1016/j.pharmthera.2020.107498
12. Yoon CI, Ahn S-G, Cha Y-J, et al. Metastasis risk assessment using BAG2 expression by cancer-associated fibroblast and tumor cells in patients with breast cancer. *Cancers*. 2021;13(18):4654. doi:10.3390/cancers13184654
13. Hou M, Yue M, Han X, et al. Comparative analysis of BAG1 and BAG2: insights into their structures, functions and implications in disease pathogenesis. *Int Immunopharmacol*. 2024;143(Pt 1):113369. doi:10.1016/j.intimp.2024.113369
14. Arndt V, Daniel C, Nastainczyk W, et al. BAG-2 acts as an inhibitor of the chaperone-associated ubiquitin ligase CHIP. *Mol Biol Cell*. 2005;16(12):5891–5900. doi:10.1091/mbc.e05-07-0660
15. Sun L, Chen G, Sun A, et al. BAG2 promotes proliferation and metastasis of gastric cancer via ERK1/2 signaling and partially regulated by miR186. *Front Oncol*. 2020;10:31. doi:10.3389/fonc.2020.00031
16. Gu JJ, Deng -C-C, An Q, et al. Lactate promotes collagen expression, proliferation and migration through H3K18 lactylation-dependent stimulation of LTBP3/TGF-β1 axis in keloid fibroblasts. *J Invest Dermatol*. 2025. doi:10.1016/j.jid.2025.04.044
17. Shim J, Oh SJ, Yeo E, et al. Integrated analysis of single-cell and spatial transcriptomics in keloids: highlights on fibrovascular interactions in keloid pathogenesis. *J Invest Dermatol*. 2022;142(8):2128–2139.e11. doi:10.1016/j.jid.2022.01.017
18. Wang Y, Wang X, Zhou X, et al. Suppressive effect mediated by human adipose-derived stem cells on T cells involves the activation of JNK. *Int J Mol Med*. 2019;43(1):177–184. doi:10.3892/ijmm.2018.3953
19. Aoki M, Matsumoto NM, Dohi T, et al. Direct delivery of apatite nanoparticle-encapsulated siRNA targeting TIMP-1 for intractable abnormal scars. *Mol Ther Nucleic Acids*. 2020;22:50–61. doi:10.1016/j.omtn.2020.08.005
20. Ma T, Tian X, Zhang B, et al. Low-dose metformin targets the lysosomal AMPK pathway through PEN2. *Nature*. 2022;603(7899):159–165. doi:10.1038/s41586-022-04431-8
21. Wang X, Ma Y, Gao Z, et al. Human adipose-derived stem cells inhibit bioactivity of keloid fibroblasts. *Stem Cell Res Ther*. 2018;9(1):40. doi:10.1186/s13287-018-0786-4
22. Luo Y, Wang D, Yuan X, et al. Oleanolic acid regulates the proliferation and extracellular matrix of keloid fibroblasts by mediating the TGF -β1/SMAD signaling pathway. *J Cosmet Dermatol*. 2023;22(7):2083–2089. doi:10.1111/jocd.15673
23. Macarak EJ, Wermuth PJ, Rosenbloom J, et al. Keloid disorder: fibroblast differentiation and gene expression profile in fibrotic skin diseases. *Exp Dermatol*. 2021;30(1):132–145. doi:10.1111/exd.14243
24. Liu F, Yu T, Liu J, et al. IGFBP-7 secreted by adipose-derived stem cells inhibits keloid formation via the BRAF/MEK/ERK signaling pathway. *J Dermatol Sci*. 2023;111(1):10–19. doi:10.1016/j.jdermsci.2023.05.004
25. Zheng D, Wei Z, Zhang C, et al. ZNF692 promotes osteosarcoma cell proliferation, migration, and invasion through TNK2-mediated activation of the MEK/ERK pathway. *Biol Direct*. 2024;19(1):28. doi:10.1186/s13062-024-00472-3
26. Zhao H, Bo Q, Wu Z, et al. KIF15 promotes bladder cancer proliferation via the MEK–ERK signaling pathway. *Cancer Manag Res*. 2019;11:1857–1868. doi:10.2147/CMAR.S191681
27. Xu DQ, Yuan X-J, Toyoda H, et al. Anti-tumor effect of Huaier extract against neuroblastoma cells in vitro. *Int J Med Sci*. 2021;18(4):1015–1023. doi:10.7150/ijms.48219
28. Liu Y, Cheng Y, Huang G, et al. Preclinical characterization of tunlametinib, a novel, potent, and selective MEK inhibitor. *Front Pharmacol*. 2023;14:1271268. doi:10.3389/fphar.2023.1271268
29. Ueda K, Kosako H, Fukui Y, et al. Proteomic identification of Bcl2-associated athanogene 2 as a novel MAPK-activated protein kinase 2 substrate. *J Biol Chem*. 2004;279(40):41815–41821. doi:10.1074/jbc.M406049200
30. Coraggio F, Bhushan M, Roumeliotis S, et al. Age-progressive interplay of HSP-proteostasis, ECM-cell junctions and biomechanics ensures C. elegans astroglial architecture. *Nat Commun*. 2024;15(1):2861. doi:10.1038/s41467-024-46827-2

31. Ogawa R, Okai K, Tokumura F, et al. The relationship between skin stretching/contraction and pathologic scarring: the important role of mechanical forces in keloid generation. *Wound Repair Regen*. 2012;20(2):149–157. doi:10.1111/j.1524-475X.2012.00766.x
32. Hsu CK, Lin -H-H, Harn HI, et al. Caveolin-1 controls hyperresponsiveness to mechanical stimuli and fibrogenesis-associated RUNX2 activation in keloid fibroblasts. *J Invest Dermatol*. 2018;138(1):208–218. doi:10.1016/j.jid.2017.05.041
33. Feng F, Liu M, Pan L, et al. Biomechanical regulatory factors and therapeutic targets in keloid fibrosis. *Front Pharmacol*. 2022;13:906212. doi:10.3389/fphar.2022.906212
34. Huang C, Liu L, You Z, et al. Managing keloid scars: from radiation therapy to actual and potential drug deliveries. *Int Wound J*. 2019;16(3):852–859. doi:10.1111/iwj.13104
35. Ding H, Chen J, Qin J, et al. TGF-β-induced α-SMA expression is mediated by C/EBPβ acetylation in human alveolar epithelial cells. *Mol Med*. 2021;27(1):22. doi:10.1186/s10020-021-00283-6
36. Rendon A, Schäkel K. Psoriasis pathogenesis and treatment. *Int J Mol Sci*. 2019;20(6):1475. doi:10.3390/ijms20061475
37. Feng Y, Lu Y. Advances in vitiligo: update on therapeutic targets. *Front Immunol*. 2022;13:986918. doi:10.3389/fimmu.2022.986918
38. Brunner PM, Guttman-Yassky E, Leung DY. The immunology of atopic dermatitis and its reversibility with broad-spectrum and targeted therapies. *J Allergy Clin Immunol*. 2017;139(4s):S65–s76. doi:10.1016/j.jaci.2017.01.011
39. Guo W, Wang H, Li C. Signal pathways of melanoma and targeted therapy. *Signal Transduct Target Ther*. 2021;6(1):424. doi:10.1038/s41392-021-00827-6
40. Luo J, Wang J, Yang J, et al. Saikosaponin B1 and Saikosaponin D inhibit tumor growth in medulloblastoma allograft mice via inhibiting the Hedgehog signaling pathway. *J Nat Med*. 2022;76(3):584–593. doi:10.1007/s11418-022-01603-8
41. Dong H, Shao M, Dong H, et al. Nanodrug rescues liver fibrosis via synergistic therapy with H(2)O(2) depletion and Saikosaponin b1 sustained release. *Commun Biol*. 2023;6(1):184. doi:10.1038/s42003-023-04473-2
42. Kar SS, Gharai SR, Sahu SK, et al. The current landscape in the development of small-molecule modulators targeting sphingosine-1-phosphate receptors to treat neurodegenerative diseases. *Curr Top Med Chem*. 2024;24(28):2431–46.
43. Komm BS, Kharode YP, Bodine PVN, et al. Bazedoxifene acetate: a selective estrogen receptor modulator with improved selectivity. *Endocrinology*. 2005;146(9):3999–4008. doi:10.1210/en.2005-0030
44. Soares-Lopes LR, Soares-Lopes IM, Filho LL, et al. Morphological and morphometric analysis of the effects of intralesional tamoxifen on keloids. *Exp Biol Med*. 2017;242(9):926–929. doi:10.1177/1535370217700524